

Analysis and Optimization of Medical Ultrasound Imaging Using the Effective Aperture Approach

Milen Nikolov, Vera Behar

Institute for Parallel Processing, Bulgarian Academy of Science, 1113 Sofia

E-mails: milenik@bas.bg; behar@bas.bg

Abstract. *An effective aperture approach is used as a tool for analysis and parameter optimization of mostly known ultrasound imaging systems – phased array systems, compounding systems and synthetic aperture imaging systems. Both characteristics of an imaging system, the effective aperture function and the corresponding two-way radiation pattern, provide information about two the most important parameters of images produced by an ultrasound system – lateral resolution and contrast. Therefore, in the design, optimization of the effective aperture function leads to optimal choice of such parameters of an imaging systems that influence on lateral resolution and contrast of images produced by this imaging system. The numerical results show that Hamming apodization gives the best compromise between the contrast of images and the lateral resolution produced by a conventional phased array imaging system. In compound imaging, the number of transducers and its spatial separation should be chosen in result of optimization of the effective aperture function of a system. It is shown that the effective aperture approach can be also used for optimization of a sparse synthetic transmit aperture (STA) imaging system. A new two-stage algorithm is proposed for optimization of both the positions of the transmit elements and the weights of the receive elements. The proposed system employs a 64-element array with only four active elements used during transmit.*

Keywords: ultrasound imaging, synthetic aperture, stochastic optimization.

1. Introduction

Medical ultrasound imaging is a technique that has become much more prevalent than other medical imaging techniques since this technique is more accessible, less expensive, safe, simpler to use and produces images in real-time. However, images produced by an ultrasound imaging system, must be of sufficient quality to provide

accurate clinical interpretation. The most commonly used image quality measures are spatial resolution, image contrast and frame rate. The two first image quality measures (resolution and contrast) can be determined in terms of beam characteristics of an imaging system beam width and side lobe level. In the design of an imaging system, the optimal set of system parameters is usually found as a tradeoff between the lowest sidelobe peak and the narrowest beam width of an imaging system. In a conventional ultrasound imaging system, the transducer is a phased array with a great number of elements (PA imaging systems). The quality of images produced by a PA system directly depends on the number of active channels used both in transmit and receive. Thus, the conventional high-resolution PA imaging systems produce images at the relatively high cost [1].

Ultrasound images produced by conventional PA imaging systems are degraded by coherent wave interference, known as “speckle”. Speckle appear as intensity variations imposed on the image due to the interference of echoes from tissue. Speckle reduce image contrast and the obtainable details within the tissue. One of basic approaches for speckle removing and contrast improving is the *Spatial Compounding* of images. This approach includes methods in which several partially correlated or non-correlated images are taken from the same region of interest (ROI) and combined together to form a single image. Decorrelation of individual images is obtained through image formation by transducers with different spatial location (*spatial compounding*) [2-4].

Conventional phased array imaging systems employ all elements of the transducer during both transmit and receive during each excitation cycle, while employing delays in order to steer the beam and scan a 2D plane. In the receive mode, dynamic (or composite) focus is used, by adjusting the delays of transducer elements as a function of the depth being imaged. In the transmit mode, usually the focus point is set in the middle of the region being imaged. At the focus point, the lateral beamwidth is the smallest (and the best lateral resolution is obtained there) while away from the focus point, the lateral beamwidth increases. The spatial resolution of the ultrasound image can be improved by using several transmit beams during the interrogation of each sector, each of which is focused at a different depth. It is done in modern ultrasound imaging systems at the cost of a decrease of the frame rate, proportionally to the number of transmit foci [5]. An alternative way to obtain an appropriate spatial resolution, without the decrease of the frame rate, is to use the synthetic aperture technique. This method makes it possible to generate images with dynamic focusing, during both transmit and receive, while maintaining or even drastically decreasing the time of image acquisition.

In a classical Synthetic Aperture Focusing Technique (SAFT), only a single array element transmits and receives at each time. All the elements are excited sequentially one after the other, and the echoes received are recorded and stored in computer memory. It reduces the system complexity and the frame rate, but requires data memory for all data recordings [6]. The main disadvantage of SAFT is the low signal-to-noise ratio (SNR) and as a result, the poor contrast resolution. In a Multi-element Synthetic Aperture Focusing (MSAF) method, at each time a group of elements transmit and receive signals simultaneously [7]. The transmit beam is defocused to emulate a spherical wave. The SNR is increased compared to SAFT, in which only a single element is used in transmit and receive. In a Synthetic Transmit Aperture (STA) method, at each time one array elements transmits a pulse, and all elements receive

the echo signals [8]. Compared to conventional phased array imaging, the advantage of this approach is that a full dynamic focusing can be applied to the transmit and the receive, producing the highest quality of images at the increased frame rate. The shortcoming is that a huge data memory is required for data recordings. For an N -element array, N echo recordings are required to form a conventional phased array image, and, however, $N \cdot N$ echo recordings are required to synthesize a STA image. This disadvantage can be overcome to some extent, if only a few elements, M , act as transmitters. In that case $M \cdot N$ echo recordings are required to synthesize a STA image, where $M < N$ [9]. This is equivalent to using of a sparse array in transmit. The sparse STA imaging acquires images at higher frame rates, which makes this method very attractive for real-time 3D ultrasound imaging.

The relation between the employed effective aperture function and the resultant radiation pattern of the imaging system can be used as a strategy for analysis and for optimisation of an imaging system [10]. Since the two-way radiation pattern of a system is the Fourier transform of the effective aperture function, the transmit and receive radiation patterns can be optimised by selecting the appropriate transmit and receive aperture functions, to produce the “desired” effective aperture of the imaging system. Thus, when the desired effective aperture of a system is defined, it also provides the two-way radiation pattern that should be used, with the appropriate width of the main-lobe and its sidelobes. In synthetic aperture imaging, the transmit aperture function depends not only on the number of transmit elements, but also on their geometrical locations within the array (sparse synthetic aperture imaging). The receive aperture function depends on the length of a physical array and the apodization weights applied to the receiver elements. Thus, the shape of the effective aperture function and, therefore, the shape of the two, one-way radiation patterns of a system, can be optimised depending on the positions of the element in transmit and the weights of the element in receive. In compounding imaging, the two-way radiation pattern depends not only on the apodization weights applied to the transmitter/receiver elements but also on the lateral or angular separation between particular transducers. Thus, the shape of the two-way radiation pattern of a compounding imaging system can be optimised depending on the weights of the array element of each transducer in transmit and receive and the lateral (angular) separation between transducers.

In this paper, it is shown how the effective aperture approach can be used for analysis and parameter optimisation of an ultrasound imaging system. Using this approach, the optimal set of system parameters (number of array elements, their configuration within an array and separation between transducers) can be determined in result of a compromise between the lowest sidelobe peak and the narrowest beam width of the two-way radiation pattern of an imaging system. The comparison analysis of 6 types of imaging systems is done calculating their effective aperture function and the corresponding two-way radiation pattern using the computational environment of Matlab.

2. The effective aperture concept

The effective aperture of an array represents an equivalent aperture that would produce an identical two-way radiation pattern if the transmit aperture were a point source. An expression for the effective aperture of an array can be derived from a calculation of the two-way radiation pattern. Consider an uniformly spaced linear array of N

elements with weighting $w(m)$, $m = 0, \dots, N - 1$. The one-way far field beam pattern is

$$(1) \quad W(\theta) = \sum_{m=0}^{N-1} w(m) e^{-j k^0 m d \sin(\theta)},$$

where d and k^0 are the inter-element spacing and the wave number, respectively. This equation can also be described as a discrete Fourier transform (DFT) of the aperture function:

$$(2) \quad W(k) = \text{DFT}[w(m)] = \sum_{m=0}^{N-1} w(m) e^{-j \frac{2\pi}{N} km}, \quad k=0, 1, \dots, N-1,$$

in which the frequency index k maps into the beam angle θ by $\sin\theta = k\lambda/Nd$ where λ is the wavelength.

Since the round-trip beam pattern is the product of the transmit and receive beams

$$(3) \quad W_{\text{RT}}(\theta) = W_{\text{R}}(\theta) W_{\text{T}}(\theta),$$

using the DFT property, we get

$$(4) \quad W_{\text{RT}}(k) = \text{DFT}[w_{\text{R}} \otimes w_{\text{T}}],$$

where \otimes denotes convolution and w_{R} and w_{T} are the apodization functions applied to the array elements in transmit and receive, respectively. Using (4), the effective aperture function of an imaging system is defined as

$$(5) \quad e_{\text{RT}} = w_{\text{R}} \otimes w_{\text{T}} \quad \text{and} \quad W_{\text{RT}}(\theta) = \text{FFT}(e_{\text{RT}}).$$

Thus, the round trip beam pattern is determined by the transmit and the receive aperture weightings. Every physical beam can be realized by forming the appropriate effective aperture.

3. Phased array imaging

Phased array is the conventional imaging system and employs a linear array transducer with N elements. All elements transmit and receive the echoes on every excitation. Both image parameters, lateral resolution and contrast, can be optimized as a function of the number of transducer elements and the apodization coefficients applied to the array elements in transmit and receive. In the transmit mode, a typical focus point is set in the middle of the view region. In the transmit mode, however, a dynamic focusing is applied providing images of a relatively good spatial resolution due to the application of dynamic focusing in receive mode. Since all the elements transmit and receive the echoes, and according to the DFT property, the round – trip beam pattern of the phased array imaging system can be found by (5): According to (5), the shape of the two-way radiation pattern depends on the number of array elements (N) and the apodization functions w_{T} and w_{R} applied to the transmit and receive elements, respectively. The contrast of ultrasound images is determined by the side lobe level of the beam pattern and can be improved by applying appropriate apodization coefficients to the transducer's elements. The lateral resolution, however, is determined

by the main lobe width of the beam pattern of the “transmitter-receiver” pair. So the apodization should be carefully chosen as a compromise between beam width and side lobe level. Another way of improving the beam width is to increase the number of elements of the transducer.

4. Compound imaging

Ultrasound images are degraded by coherent wave interference, known as “speckle”. It reduces the image contrast and detail resolution. Spatial compounding proves to be an efficient technique for reducing the speckle noise. It is a technique in which several images are taken from the same area and combined together to form a single image. In this paper, we study the compounding imaging system that employs three or more different transducers, each of them with N elements. Each transducer takes an image of the same area and then the images are combined together to form an output image. Depending on the strategy used for combining the images, the lateral resolution, the contrast, and the SNR can be improved. The images are taken from different lines of sight, so the speckle signal de-correlates and is suppressed by the averaging operation. Provided the registration of the scan planes is accurate, the averaging operation will highlight only the real objects. Theoretically, for fully developed speckle in a single-angle image, the SNR can reach 1.91. If compounding M independent images, SNR can theoretically reach $1.91\sqrt{M}$. We use the effective aperture approach for optimal choice of a compounding strategy with aim to obtain the best lateral resolution and contrast of images. Let’s consider three transducers. Each transducer takes an image of the area of interest, so there are three different images which have to be combined (Fig. 1). The transducers are prefocused with the same focus point F . The reflected signal, coming from the direction of this point, is received with maximum of the main lobe of the corresponding transducer’s beam. Any other point lies away from the focus point and the angles between it and the transducers are different. The angle between transducer 1, which is the central transducer, and point A is θ . For transducers 2 and 3 the corresponding angles are:

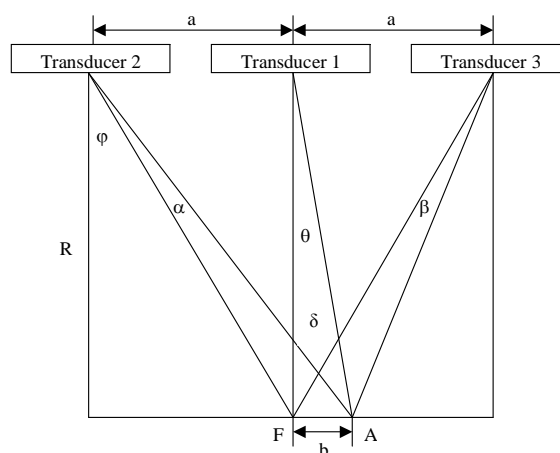


Fig. 1. Compound imaging method

$$(6) \quad \alpha = \arctg[(a+b)/R] - \varphi \quad \text{and} \quad \beta = \varphi - \arctg[(a-b)/R],$$

where a is the distance between transducers' centers, b – the distance between the focal point F and the current point A , and R is the focus. The angle between the transducers φ is calculated as

$$(7) \quad \varphi = \arctg(a/R).$$

These formulas can be used for finding the corresponding points in the transducers' beam patterns. Then these points can easily be combined using appropriate combining strategy. The compounding two-way radiation pattern is calculated as a function

$$(8) \quad W(\theta) = \text{Compoundin g} \{W_1(\theta), W_2(\alpha), W_3(\beta)\},$$

where W_1 , W_2 and W_3 are the two-way radiation patterns of the three transducers and have the form:

$$(9) \quad W_1 = \text{FFT}(w_{T,1} \otimes w_{R,1}), \quad W_2 = \text{FFT}(w_{T,2} \otimes w_{R,2}) \quad \text{and} \quad W_3 = \text{FFT}(w_{T,3} \otimes w_{R,3}).$$

Using (8) and (9), the shape of $W(\theta)$ can be optimized depending on the parameters of each transducer and the compounding strategy.

5. Synthetic aperture imaging

First, the concept of synthetic aperture was originally used in radar for highly resolution imaging terrain, but it can be successfully used in ultrasound imaging systems as well. In this case, the benefit of the synthetic aperture is the reduction of system complexity and cost. Several methods were proposed to form a synthetic aperture for ultrasonic imaging. In SAFT imaging, at each time only a single array element transmits a pulse and receives the echo signal (Fig. 2). The system complexity is reduced, because only a single set of circuit for transmit and receive is needed. In this case the effective aperture can be calculated by

$$(10) \quad e_N = \sum_{m=1}^N w_R(m) w_T(m), \quad \text{where} \quad w_R(m) = w_T(m) = [0, 0, \dots, i_m, \dots, 0] \quad \text{and} \quad i_m = 1.$$

In MSAF imaging, a group of elements transmit and receive signals simultaneously, and transmit beam is defocused to emulate a single element response (Fig. 3). The acoustic power and the signal-to-noise ratio are increased compared to

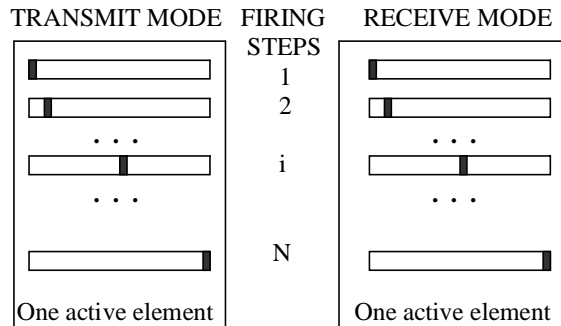


Fig. 2. SAFT imaging method

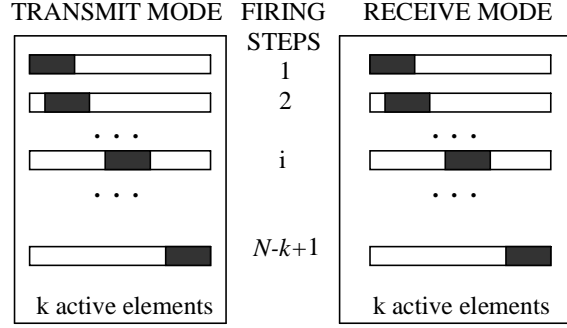


Fig. 3. MSAF imaging method

SAFT where a single element is used. This method requires also memory for data recordings. In MSAF, a K_T -element transmit subaperture sends an ultrasound pulse and echo signals are recorded at a K_R -element receive subaperture. At the next step, one element is dropped and a new element is included to the transmit and receive subaperture, repeating the transmit and receive process. Usually $K_T=K_R=k$. The effective aperture is

$$(11) \quad e_N = \sum_{m=1}^{N-k+1} w_R(m) w_T(m),$$

where

$$w_R(m) = w_T(m) = [0, 0, \dots, i_m, i_{m+1}, \dots, i_{m+k-1}, 0, \dots, 0], \quad i_m = i_{m+1} = \dots = i_{m+k-1} = 1.$$

In STA imaging, at each time one array element transmits a pulse and all elements receive the echo signals (Fig. 4). The advantage of this approach is that a full dynamic focusing can be applied to the transmit and the receive, giving the highest quality of image. The disadvantage is that a huge data memory is required and motion artifacts may occur. The effective aperture is calculated as:

$$(12) \quad e_N = \sum_{m=1}^N w_R w_T(m) \quad \text{where} \quad w_R = [1, 1, \dots, 1], \quad w_T(m) = [0, 0, \dots, i_m, \dots, 0] \quad \text{and} \quad i_m = 1.$$

Synthetic Receive Aperture (SRA) method of imaging was proposed to improve lateral resolution (Fig. 5). It is known that the lateral resolution can be improved by increasing array length. In practice, it is not very expensive to build a large transmit aperture, but is very complex to form a large receive aperture. This method uses a large transmit aperture and enables an imaging system to address a large number of transducer receive

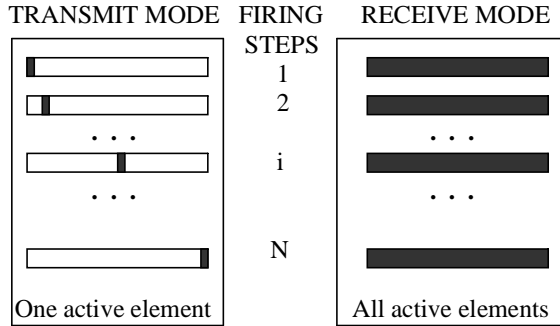


Fig. 4. STA imaging method

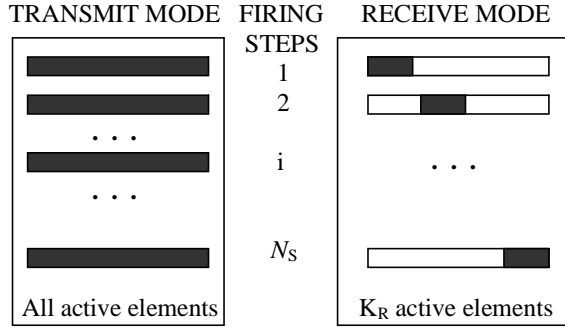


Fig. 5. SRA imaging method

elements without the same number of parallel receive channels. In the receive mode, the aperture is split into two or more subapertures. In order to form each line of image data in the SRA system, the transmitters must be fired once for each receive subaperture. For a single transmit pulse (from all transmit elements), the RF sum for one receive subaperture is formed and stored in memory. Then a second identical pulse is transmitted in the same direction and the RF sum for another subaperture is formed and stored. After the RF signals have been acquired from all receive subapertures, the total RF sum is formed by coherently adding together the sums from various subapertures. For an N -element linear array, receive aperture is split into $N_S = N/K_R$ subapertures, and each subaperture contains K_R elements. The effective aperture is:

$$(13) \quad e_N = \sum_{m=0}^{N_S-1} w_R(m) w_T, \text{ where}$$

$$w_T = [1, 1, \dots, 1], \quad w_R(m) = [0, 0, \dots, i_n, i_{n+1}, \dots, i_{n+K_R-1}, 0, \dots, 0],$$

$$n = mK_R + 1, \quad n = mK_R + 1.$$

A sparse STA imaging method is proposed to increase system frame rate (Fig. 6). Only a small number of elements are used to transmit a pulse but all array elements receive the echo signals. For an N -element aperture, $M \times N$ data recordings are needed for image reconstruction., where $M \ll N$. All data recordings must then be combined with dynamic focusing. The effective aperture is:

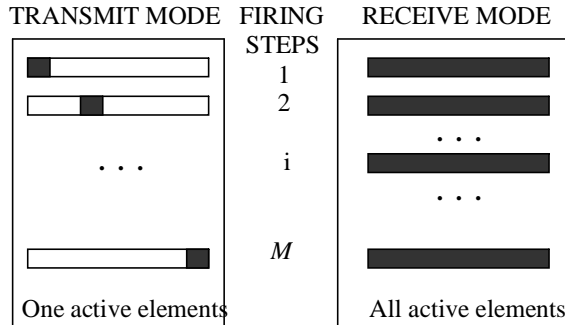


Fig. 6. Sparse STA imaging method

$$(14) \quad e_N = \sum_{m=1}^M w_T(m) \otimes w_R,$$

where $w_T(m) = [0, 0, \dots, i_{K_m}, \dots, 0]$, $w_R = [1, 1, \dots, 1]$ and $i_{K_m} = 1$.

The two-way radiation pattern of a synthetic aperture imaging system is calculated using the Fourier transform of the corresponding effective aperture function defined by the expressions (10)-(14).

6. Optimization of a sparse array

For a sparse STA imaging system with an array with N -elements, the two-way radiation pattern is evaluated as the Fourier Transform of the effective aperture function e_N , defined as:

$$(15) \quad e_N = \sum_{m=1}^M a_m \otimes B, \quad \text{and} \quad a_m = [0, 0, \dots, i_m, \dots, 0], \quad i_m = 1,$$

where a_m is the transmit aperture during the m -th firing, B is the apodization function applied to the receiver elements, and \otimes is the convolution operator. The speed of the image acquisition is determined by the number of transmit elements (M), $M \ll N$. Since the geometrical locations of the transmit elements in a sparse array system impact the two-way radiation pattern of that system, the image quality parameters, the lateral resolution and contrast, all depend on the locations of the transmit elements within the sparse array (i_1, i_2, \dots, i_M). Since the weighting applied to each receiver element also impacts the radiation pattern of the system, the image quality also depends on the type of the apodization function (B). Therefore, the optimization of a sparse STA imaging system can be formulated as an optimization problem of both the location of the elements of the sparse array in transmit and the weights assigned to the elements of the full array during receive [11]. Different algorithms have been proposed for optimization of the locations of the transmit elements in a sparse array – genetic, linear programming and simulated annealing algorithms [11]. For most cases the optimization criterion is minimal sidelobe peak of the radiation pattern.

In this paper, another optimization criterion is proposed. It is the minimal width of the mainlobe (W) combined with a condition on the maximum sidelobe level ($SL < Q$). It is suggested here to divide the optimization process into two stages. In the first stage, the optimal positions of transmit elements ((i_1, i_2, \dots, i_M)) are found, for a set of known apodization functions $\{B_k\}$, $k=1, 2, \dots, K$. Such a set of apodization functions may include several well-known window-functions (Hamming, Hann, Kaiser, Chebyshev and etc). At this stage, the optimization criterion can be written as follows:

(16) Given M, N and $\{B\}_K$, choose $(i_1, i_2, \dots, i_M)_K$ to minimize W subject to $SL < Q$, where Q is the threshold of acceptable level of the sidelobe peak. In the second stage, the final layout of transmit elements is chosen, which is a layout that corresponds to the most appropriate apodization function $B = (b_1, b_2, \dots, b_N)$. This choice is a compromise between minimal width of the mainlobe and the acceptable level of the peak of the sidelobes. Mathematically, it can be written as follows:

- (17) Given $M, N, \{B\}_K$ and $\{i_1, i_2, \dots, i_M\}_K$, choose (b_1, b_2, \dots, b_N)
to minimize W subject to $SL < Q$,

where $\{i_1, i_2, \dots, i_M\}_K$ are the selected positions of transmit elements, as found at the first stage of the optimization.

One way of selecting the positions $\{i_1, i_2, \dots, i_M\}_K$ is by using a modification of the simulated annealing algorithm based on a Monte Carlo simulation. This approach was suggested initially for combinatorial optimization by Kirkpatrick et al. [12]. The simulated annealing algorithm realizes an iterative procedure that is determined by simulation of the arrays with variable transmit element positions. In order to speed up the simulation process it is assumed that two of the M transmit elements are always the two outer elements of the physical array; their positions are not changed and are assigned numbers 1 and N . The positions of the other transmit elements are shifted randomly, where a shift in position to the left or to the right has equal probability (of 0.5). Once the process is initiated, with an initial layout of transmit elements $I_0 = (i_1^0, i_2^0, \dots, i_M^0)$, a neighbor layout $I_1 = (i_1^1, i_2^1, \dots, i_M^1)$ is generated, and the algorithm accepts or rejects this layout according to a certain criterion. The acceptance is decided stochastically and may be described in terms of probability as:

$$(18) \quad P = \begin{cases} 1 & \text{if } \Delta W < 0 \text{ \& } \Delta SL < 0, \\ \exp(-\Delta W / T_k) & \text{if } \Delta W > 0 \text{ \& } \Delta SL < 0, \\ \exp(-\Delta SL / T_k) & \text{if } \Delta W < 0 \text{ \& } \Delta SL > 0, \\ \exp(-\Delta W / T_k) \exp(-\Delta SL / T_k) & \text{if } \Delta W > 0 \text{ \& } \Delta SL > 0, \end{cases}$$

where P is the probability of acceptance, ΔW is the difference of width of the mainlobe, ΔSL is the difference of the height of the peak of the sidelobe between the current configuration of transmit elements and the best one obtained at preceding steps. T_k is the current value of 'temperature', where the current 'temperature' is evaluated as $T_k = 0.95 T_{k-1}$, and the algorithm proceeds until the number of iterations reaches the

```

begin
  Initialize ( $I_0, T_0$ )
  for  $k=1$  to number_iterations
     $T_k = T_k \cdot \alpha$ 
    for  $j=1$  to number_perturbations
       $I_p = \text{perturbate}(I_{j-1})$ 
       $\Delta W = W(I_p) - W(I_{j-1})$ 
       $\Delta SL = SL(I_p) - Q$ 
      if  $\{\Delta W < 0 \text{ or } \exp(-\Delta W / T_k) < \text{rand}(0, 1)\}$ 
        &
         $\{\Delta SL < 0 \text{ or } \exp(-\Delta SL / T_k) < \text{rand}(0, 1)\}$ 
           $I_j = I_p$ 
        else
           $I_j = I_{j-1}$ 
        endif
      endfor
    endfor
  end

```

Fig .7. The simulated annealing algorithm

final value. A pseudo-code of the proposed simulated annealing algorithm is given in Fig.7.

7. Computations and comparison analysis

The effective aperture function and the corresponding two-way radiation pattern of several ultrasound imaging systems were calculated using Eqns. (1)-(18), in order to compare the quality of images produced by the questioned systems.

Phased array imaging. The conventional phased array systems with 128, 64 and 32 elements are investigated depending on the apodization function applied to the array elements in transmit and receive (Table 1). The following apodization functions are investigated: Boxcar window (i.e. no apodization) – Fig.8 and Fig.9, Hamming window – Fig. 10, Blackman window – Fig. 11 and Chebyshev window – Fig. 12. The image quality was expressed in terms of the lateral resolution (-6dB -beamwidth) and the contrast (peak of side lobes $-SL$). The results show that a larger aperture has better lateral resolution and practically the same SL. Using of apodization degrades the lateral resolution, but SL falls down significantly. The Hamming window is a good compromise decision since the resolution is not degraded much. The SL is below -85 dB and this is quite sufficient.

Table 1. Mainlobe width and sidelobe peak level of a phased array imaging system

Number of elements	Apodization							
	No Apodization		Hamming		Blackman		Chebyshev, $r=50$	
	$\Delta\theta, ^\circ$	SL, dB	$\Delta\theta, ^\circ$	SL, dB	$\Delta\theta, ^\circ$	SL, dB	$\Delta\theta, ^\circ$	SL, dB
128	0.6815	-26.996	1.0985	-85.339	1.4067	-116.65	1.1207	-100
64	1.3568	-27.061	2.2088	-85.279	2.8379	-116.88	2.2560	-100
32	2.6896	-27.187	4.466	-84.988	5.778	-117.54	4.5606	-100

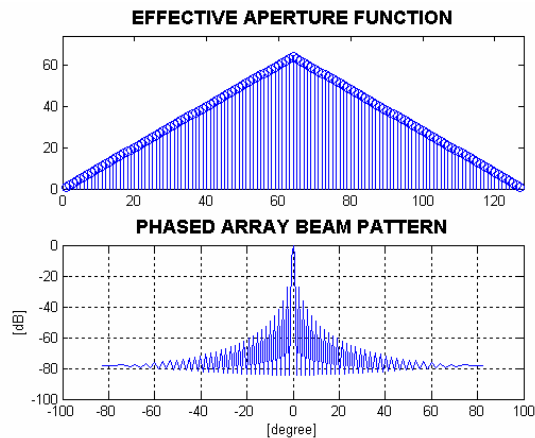


Fig. 8. 64-element phased array without apodization

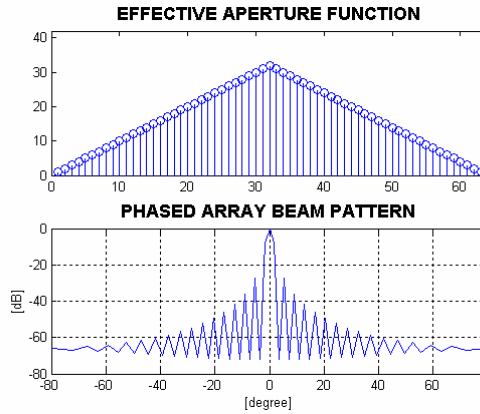


Fig. 9. 32-element phased array without apodization

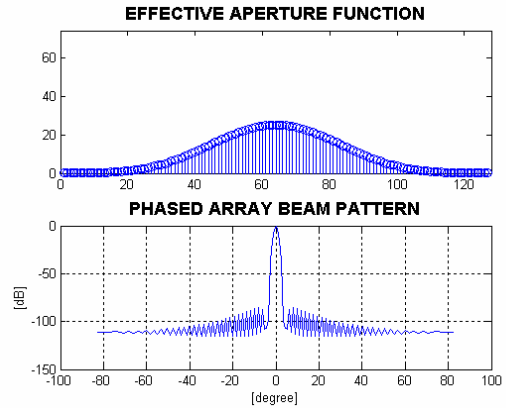


Fig. 10. 64 element-phased array (Hamming apodization)

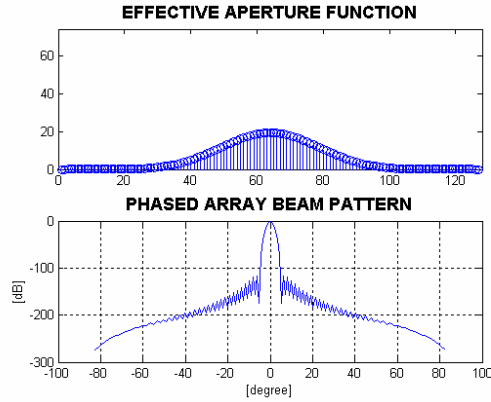


Fig. 11. 64 element-phased array (Blackman apodization)

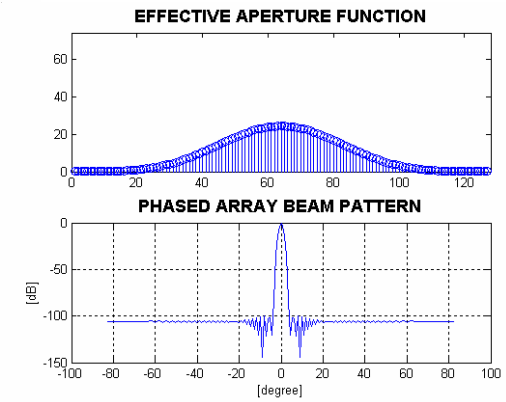


Fig. 12. 64-element phased array (Chebyshev apodization)

Compound imaging. The compounding system is composed of 3, 5 or 7 transducers (Table 2), with separation distance between the transducers equal to the distance R between the main transducer and the focal point F , i.e. $a=R$ (Fig. 1). For the system with 3 transducers, experiments are made with two other separation distances – minimal separation distance – equal to the length of the transducer (angle

Table 2. Mainlobe width of a compound imaging system

Compounding Strategy	Number of transducers, (separation distance between transducers = R)			Angle between transducers, 3 transducers (δ)		
	3	5	7	18.1716°	45°	63.4349°
Mean($A_1, A_2, \dots, A_{n-1}, A_0$)	3.6269	4.9312	7.2086	2.3025	3.6269	6.4842
Median($A_1, A_2, \dots, A_{n-1}, A_0$)	4.3322	4.4897	10.5965	2.3410	4.3322	10.5965
$(A_1 A_2 \dots A_{n-1} A_0)^{1/n}$	3.1475	3.8895	4.4210	2.2993	3.1475	3.6476
$A_1 A_2 \dots A_{n-1} A_0$	1.5517	1.2941	1.1941	1.1071	1.5517	1.9653
A_0 (no compounding)	2.2088					

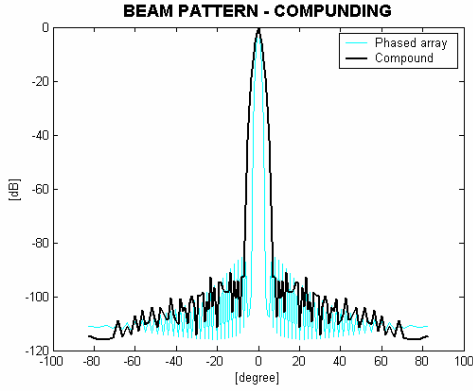


Fig. 13. Compounding method
 $A_{\text{comp}} = \text{mean}(A_1, A_2, \dots, A_{n-1}, A_0)$;
 3 transducers, separation angle 45°

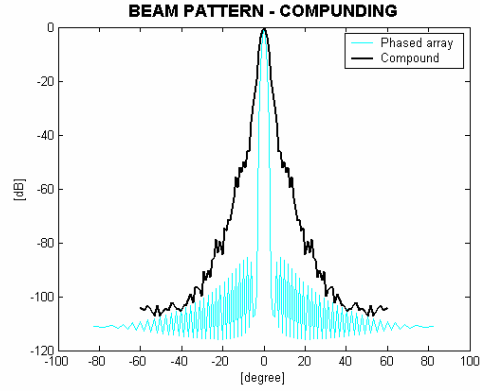


Fig. 14. Compounding method
 $A_{\text{comp}} = (A_1 A_2 \dots A_{n-1} A_0)^{1/n}$;
 7 transducers, separation angle 45°

separation between the transducers is $\delta=18.1716^\circ$), and separation distance of $2R$ (angle separation between the transducers is $\delta=63.4349^\circ$). Each transducer is of 64 active elements, and Hamming window is applied to the transducer's elements in transmit and receive. The following compounding strategies are used to form a compounded image: (i) $A_{\text{comp}} = \text{mean}(A_1, A_2, \dots, A_{n-1}, A_0)$, where A_0 corresponds to the signal intensity obtained from the central transducer and A_i – from the other transducers (Fig. 13); (ii) $A_{\text{comp}} = \text{median}(A_1, A_2, \dots, A_{n-1}, A_0)$; (iii) $A_{\text{comp}} = (A_1 A_2 \dots A_{n-1} A_0)^{1/n}$ (Fig. 14 and Fig. 16); (iv) $A_{\text{comp}} = A_1 A_2 \dots A_{n-1} A_0$ (Fig. 14). The best lateral resolution is obtained for a system with three transducers, the minimal distance between them and the compounding strategy $A_{\text{comp}} = (A_1 A_2 \dots A_{n-1} A_0)^{1/n}$.

Synthetic aperture. Three more perspective types of synthetic aperture imaging systems are investigated.

The investigated MSAF imaging system employs a linear array with 64 elements and active sub-apertures with 4, 8 (Fig. 17), 16 (Fig. 18) or 32 elements, respectively. In the study no apodization is used. The best results for the lateral resolution and SL are obtained when the active transmit sub-aperture consists of only 4 elements

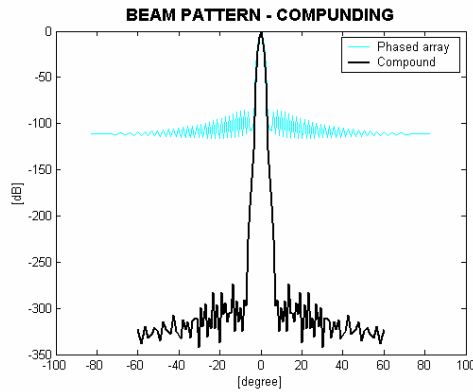


Fig. 15. Compounding method;
 $A_{\text{comp}} = A_1 A_2 \dots A_{n-1} A_0$;
 3 transducers, separation angle 45°

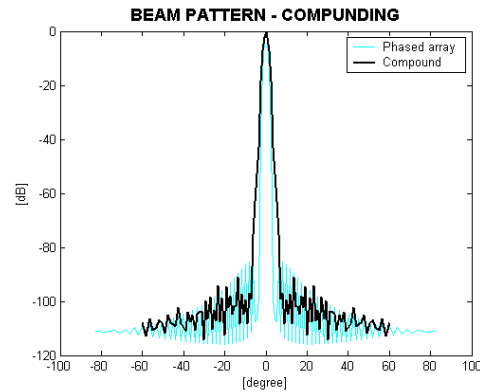


Fig. 16. Compounding method;
 $A_{\text{comp}} = (A_1 A_2 \dots A_{n-1} A_0)^{1/n}$;
 3 transducers, separation angle 45°

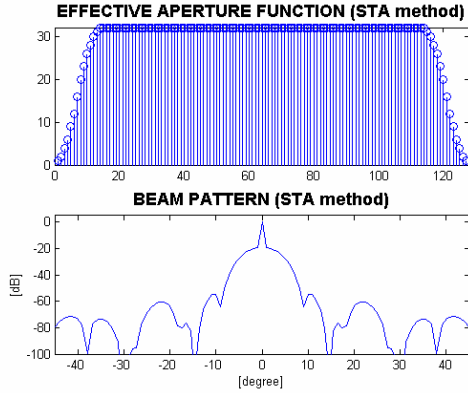


Fig. 17. MSAF method with 8 active elements

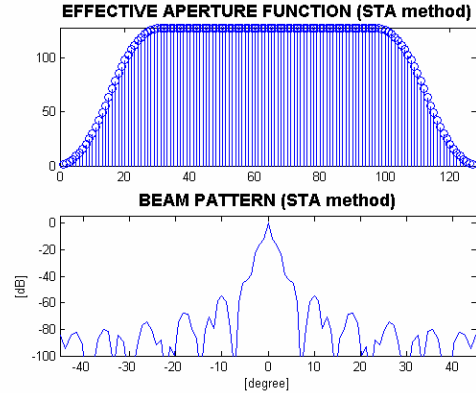


Fig. 18. MSAF method with 16 active elements

Table 3. Mainlobe and sidelobe peak level of a MSAF imaging system

Number of transmit elements	4	8	16	32
$\Delta\theta, ^\circ$	0.3896	0.5664	0.9188	1.7685
SL, dB	-59.6213	-54.3839	-54.574	-35.2764

(Table 3). The main disadvantage of the small number of active transmit elements is that the transmitted power is less, hence the SNR is low.

In a conventional STA imaging method, the transducer is of 64 elements. In the receive mode all elements are active. In the transmit mode, the linear array is split into 64 sub-apertures, each of them has only one active element. The effective aperture function and the corresponding two-way radiation pattern of such a STA imaging system is shown in Fig.19. The -6 dB beamwidth obtained for the STA imaging system is 1.82° against 2.2° for the phased array with 64 elements (Table 1). However, the sidelobe peak level of the STA system is only -32 dB against -85 dB of the phased array imaging system (Table 1).

Sparse array optimization. Computer simulations were performed in order to optimize the design and performance of a sparse array probe, to be used for synthetic transmit aperture imaging. The example given here is of a 64 elements sparse array, where 64 active elements are used in receive and only 4 elements are used in transmit. The properties of the system are optimized using the two-stage algorithm described in section 6. First, the optimal positions of transmit elements are found for three apodization functions – Boxcar (i.e. no apodization of the receiver elements), Hamming and the Blackman-Harris. For each apodization function, the positions of transmit elements are shifted until optimal performance is obtained, as described earlier, using the simulated annealing algorithm presented in Fig.7. In order to obtain a radiation pattern with a sharper mainlobe, the optimization criterion was formulated as the minimal width of the mainlobe at -20 dB (instead of at -6 dB) below the maximum where the condition that the maximal level of the sidelobe peak is below -50 dB. The positions of transmit elements that were found to optimize the performance of the system, studied for a physical array with $\lambda/2$ element spacing, together with the achieved widths of the mainlobe (at -6 dB, -20 dB and -40 dB) and the levels of the peaks of the sidelobe, are all presented in Table 4. Both optimized functions, the effective aperture function and the corresponding two-way radiation pattern, are plotted for Hamming apodization function (Fig. 20). It may be seen that the apodization

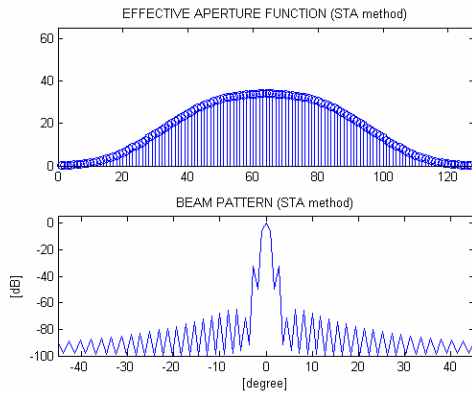


Fig.19. Conventional STA method (64 elements, Hamming apodization)

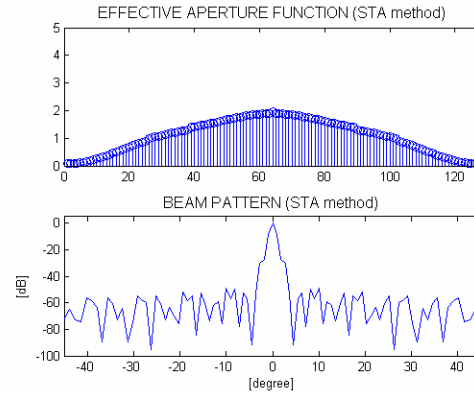


Fig. 20. Sparse STA method (4 transmit elements, 64 receive elements, Hamming apodization)

Table 4. Numerical results obtained after employing the two stages of the optimization

Optimized positions of transmit elements	Receiver apodization	Mainlobe width ($\Delta\theta$, °)			SL, dB
		-6 dB	-20 dB	-40 dB	
1, 2, 63, 64	–	0.33	1.11	3.2	-33
1, 26, 39, 64	Hamming	1.34	2.92	6.2	-50
1, 21, 44, 64	Blackman–Harris	1.32	4.33	11.16	-100

reduces the levels of the peaks of the sidelobes from -33 dB to -100 dB, but at the cost of widening the mainlobe of the radiation pattern. Since the dynamic range of a computer monitor is limited to about 50 dB, the sparse array is chosen with the Hamming apodization and the locations of the transmit elements are set to be at positions 1, 26, 39 and 64. Comparison analysis of numerical results (Table 1, Table 4, Fig. 19) shows that a sparse STA imaging system improves significantly lateral resolution of images because $\Delta\theta = 2.2^\circ$ – for a phased array system, $\Delta\theta = 1.82^\circ$ – for a conventional STA imaging system and $\Delta\theta = 1.34^\circ$ – for a sparse STA imaging system.

8. Conclusions

It is shown that the effective aperture approach can be successfully used as a tool for analysis and parameter optimization of mostly known ultrasound imaging systems – phased array systems, compounding systems and synthetic aperture imaging systems. The effective aperture function and the corresponding two-way radiation function provide information about two the most important parameters of images produced by an ultrasound system – lateral resolution and contrast. Therefore, in the design, optimization of the effective aperture function leads to optimal choice of such parameters of an imaging systems that influence on lateral resolution and contrast of images produced by this imaging system.

The numerical results show that each system has its own advantages and disadvantages. The choice of imaging system should depend on the task which it will be used for. It is shown that Hamming apodization gives the best compromise between

the contrast of images and the lateral resolution. In compound imaging, the using of more transducers and the increasing of the distance between transducers worsens the lateral resolution.

It is shown that the sparse synthetic transmit aperture imaging systems can be proposed as an alternative and superior approach to the phased array systems. Yet, the sparse STA imaging systems suffer from some deficiencies. With proper design, these deficiencies can be overcome and the sparse STA imaging system can perform extremely well for specific applications. To do so, an effective aperture approach is used for optimisation of the sparse STA imaging system. A two-stage algorithm is proposed for optimising both the locations of transmit elements within the ultrasound probe and the weights of the receive element. The first stage of the optimisation procedure employs a simulated annealing algorithm that optimises the locations of the transmit elements for a set of apodization functions. At the second stage, an appropriate apodization function is selected.

Acknowledgments. This work was supported by the Centre of Excellence BIS21⁺⁺ and the Bulgarian National Science Fund – grant MI-1506/05.

References

1. Angelsen, B. Ultrasound imaging: Waves, signals, and signal processing. Emantec, Norway, 2000.
2. Trahey, G., S. Smith, O. Van Ram. Speckle pattern correlation with lateral aperture translation: Experimental results and implications for spatial compounding. – IEEE Trans. Ultr. Ferr. Freq. Cont., Vol. **33**, 1986, 257-264.
3. Jespersen, S., J. Wilhelm, H. Sillescu. Multi-angle compounding imaging. – Ultrason. Imag., **20**, 1998, 82-102.
4. Behar, V., D. Adam, Z. Friedman. A new method of spatial compounding imaging. – Ultrasonics, **41**, 2003, 377-384.
5. Holm, S., H. Yao. Method and apparatus for synthetic transmit aperture imaging. US patent No 5.951.479, September 14, 1999.
6. Ylitalo. On the signal-to-noise ratio of a synthetic aperture ultrasound imaging method. – Europ. J. Ultras., **3**, 1996, 277-281.
7. Karaman, M., H. Bilge, M. O'Donnell. Adaptive multi-element synthetic aperture imaging with motion and phase aberration correction. – IEEE Trans. Ultrason. Ferroelec. Freq. Contr., Vol. **45**, 1998, No 4, 1077-1087.
8. Trahey, G., L. Nock. Multi-element synthetic transmit aperture imaging using temporal coding. – IEEE Trans. Med. Imag., Vol. **22**, 2003, No 4, 552-563.
9. Behar, V., D. Adam. Optimization of sparse synthetic transmit aperture imaging with coded excitation and frequency division, Ultrasonics, 2005 (to be printed).
10. Lockwood, G. R., F. S. Foster. Design of Sparse Array Imaging Systems.
11. Holm, S., A. Austen, K. Iranpour, J. Hopperstad. Sparse sampling in array processing. Chapter 19. – In: Sampling Theory and Practice. F. Marvasti, Ed., N. Y., Plenum, 2001.
12. Kirkpatrick, S., C. Gelatt, M. Vecchi. Optimization by simulated annealing. – Science, **220**, 1988, 671-680.